AIAA Propulsion and Energy Forum
19-22 August 2019, Indianapolis, IN
AIAA Propulsion and Energy 2019 Forum

10.2514/6.2019-4415

Numerical Simulation of Combustion in a Hybrid Rocket with Liquefying Fuels

Gurunadhan Mohana Durga Prasad [*]
Louisiana State University, Baton Rouge-70820

Shyam Menon[†]
Louisiana State University, Baton Rouge-70820

Adam Baran[‡]
Louisiana State University, Baton Rouge- 70820

The methodology and implementation for numerical transient analysis of combustion in a hybrid rocket with liquefying fuel is presented. In this work, both the solid-liquid and liquid-gas phase change problems are considered, by employing a decoupled model for combustion and melting phase change. All the governing equations and model implementations are carried out in the frame work of commercial software ANSYS-FLUENT. A 2-dimensional problem is solved, which involves oxidizer flow over a paraffin wax fuel slab and is compared with the experimental regression rate data. The objective of the analysis is to understand the effect of melt layer surface instability and liquid droplet entertainment on the effective vaporization rate of the fuel. The regression rate predicted by the finite rate combustion model was in close agreement with the experimental results while the Eddy dissipation model based on single step stochiometric overpredicted the regression rate. The melting model, based on temperature and vaporization input from combustion model, predicted couple of orders higher melting rate than the experimental observations. The possible reasons for this deviation and required amendments to the existing melting model are discussed in detail.

Downloaded by 184.186.21.165 on August 17, 2019 | http://arc.aiaa.org | DOI: 10.2514/6.2019-4415

Nomenclature

$\dot{m}$ = Vaporization mass flux
Y = Species mass fraction
D_g = Diffusion coefficient
κ = Thermal conductivity
L_v = Latent heat of vaporization
K_e = Equilibrium constant (reversible reaction)
Subscripts: =
n = Normal
l = liquid
s = solid
g = gas

I. Introduction

A hybrid rocket propulsion system provides an alternative to conventional solid and liquid systems. The benefits of utilizing a hybrid propulsion system are reviewed in the work of Kuo et. al [1]. Hybrid systems utilizing polymeric fuel suffer from the disadvantage of slower fuel surface regression rates. This shortcoming is significantly improved

---

[*] PhD student, Department of Mechanical and Industrial engineering

[†] Associate Professor, Department of Mechanical and Industrial Engineering

[‡] Adjunct Professor, Department of Mechanical and Industrial Engineering

Copyright © 2019 by the American Institute of Aeronautics and Astronautics, Inc. All rights reserved.

by utilizing two methodologies, involving improvements to the oxidizer flow configuration and utilizing liquefying fuel (mostly in cryogenic range) [1]. Liquefying fuel refers to the material being capable of forming a distinct melt liquid layer during the operating conditions [2]. Liquefying fuel provided approximately 10 folds improvement in the regression rate, without any major structural modifications, thus being a popular choice for replacing the conventional systems [1].

The use of various liquefying fuels for hybrid combustion was studied in the work of Larson et. al [3] and Gramer et. al [4]. The theoretical research was propelled by the necessity to understand the mechanism behind the increased regression rates. An initial study attributed it to the lower latent heats associated with the liquefying fuels. However, the work of Karabeyoglu et. al [5, 6] attributed the increased regression rate to the liquid melt layer surface instability and ensuing fuel droplet entrainment in the oxidizer flow. One dimensional transient analysis [5] was conducted to predict the regression rate, which included the semi empirical droplet entrainment and vaporization model emulating the experimental work of Gater et. al [7]. Though the regression rate values are in good agreement with the experimental data used in their research work, the extension of these results to any general flow configuration involving arbitrary initial fuel shape and flow parameters is a subject of discussion, as entrainment and the ensuing vaporization rates are significantly influenced by the geometry of the problem. This was corroborated in the work of Venkateswaran et. al [8], who conducted numerical analysis of hybrid engine with polymeric fuel, which showed that geometric scale of the rocket affected the flow and energy gradients at the fuel surface. As an extension of their work, Karabeyoglu et. al [6] conducted a linear stability analysis, which presented a closed form solution relating the amplification rates to the flow input conditions. One of the drawbacks of a linear stability analysis is that it is utilized only to obtain a qualitative estimation of the best operating regime and cannot provide the exact fuel surface conditions, which is essential for prediction of regression rates.

Owing to the limitations with analytical modeling and development time, complexity associated with developing a experimental setup, a comprehensive numerical methodology is preferable, which will obviate the shortcomings and is capable of providing an insight into the interfacial mass transfer mechanism. Several numerical analysis has been conducted on polymeric fuel (mostly HTPB) [8–12]. They share common features of using a two equation turbulence model, Arrhenius/ eddy dissipation reaction rate equation and empirical model for vapor generation at the fuel surface, where in the fuel surface is modeled as a wall and vapor generation is coded as a volumetric source term in the cell adjacent to the wall. The effect of fuel surface displacement, in the case of polymeric fuel, was included in the work of Coronetti et. al [12] where in the boundary surface nodes were displaced based on the fuel regression rate.

Experimental studies, with the objective of visualization of melting and its effect on combustion, were carried out by Petralo et. al [13], Jens et. al [14] and Chandler et. al [15]. The ensuing discussions in all the referred experimental studies predominantly involved high speed photographs highlighting transient events during initiation of combustion and liquid melt entertainment by the shearing gas layer. A quantitative description of the entrainment or the surface wave generation and its decomposition to pertinent frequency components was not discussed, this could be owing to the limitation of the employed image processing techniques.

A numerical study using liquefying propellants (Paraffin wax) was conducted by Ranuzzi et. al [16], which followed the same procedure as polymeric fuel, replacing its properties with that of the liquefying fuel, mainly detailing the application of NExT solver. In one of the recent work by Leccese et. al [2], a comprehensive study on hybrid combustion with Paraffin wax as propellant was conducted. A detailed gas-surface interaction semi-empirical model was employed and the effects of radiation were included in the analysis. Elaborate reaction steps were suggested, based on the work of Coronetti et. al [12], which includes the effect of thermal cracking. Hitherto, no research work had included the kinetic rate parameters involved in reaction steps of Paraffin wax, which was adapted from the work of Coronetti et. al [12] carried out on polymeric fuels. However, the direct simulation of phase change and fuel entrainment was not included, which was justified by the assumption of critical operating conditions.

In the present work, phase change process is directly simulated and the surface instability effects on combustion would be directly included. Melting, vaporization and combustion- three important process in a Hybrid propulsion system would be directly simulated, while employing a decoupling between combustion and melting.This will provide the possibility of numerically exploring the physics of surface wave generation and entrainment.The overall envisaged algorithm is arranged as a flowchart in Fig.1. However this paper is limited to one iteration of combustion followed by melting. In this paper, each solver, used in the methodology, is discussed in brief, followed by the description of case study involving Paraffin slab combustion. As the implementation is still in development, the preliminary results are discussed in detail, concluding with the future course of this research.

Downloaded by 184.186.21.165 on August 17, 2019 | http://arc.aiaa.org | DOI: 10.2514/6.2019-4415

Downloaded by 184.186.21.165 on August 17, 2019 | http://arc.aiaa.org | DOI: 10.2514/6.2019-4415

II. Methodology

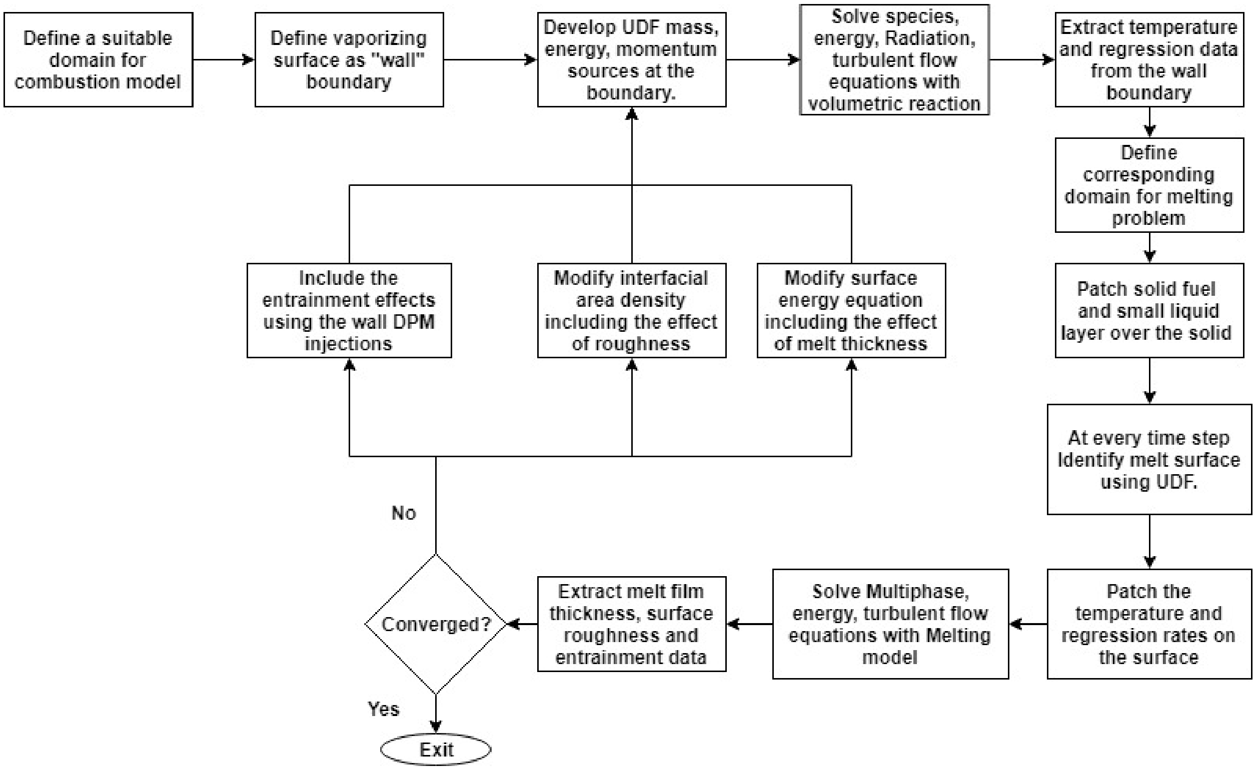

Fig. 1 Envisaged decoupled algorithm

The solvers implemented by ANSYS-Fluent are utilized for solving the relevant physics of the problem. The models used are given in Table 1.As it is essential to resolve boundary layer and free stream conditions accurately, Shear Stress Transport (SST) K-ω was chosen for turbulence modeling, which reduces the observed sensitivity of K-ω model to inlet turbulence properties.

PHYSICS	MODEL/TECHNIQUE
Turbulence	SST k-ω model
Melting	Enthalpy-porosity
Multiphase	Explicit VOF with PLIC interface reconstruction.
Combustion	Species equation with Eddy Dissipiation/ Laminar finite rate

Table 1 Numerical models

The effect of vaporization was included by providing a vaporization source term to the fuel melt-gas interface. This requires prediction of the interface area fluid-fluid interface , reconstructed by the methodology of Piece wise Linear Interface Construction (PLIC). A PLIC algorithm was implemented following the methodology of Scheufler et. al [17]. The overall algorithm for the source term evaluation can be summarized as:

V.1 Iteratively smooth the VOF field, by using information from nearest neighboring cells (9 cells in 2-D/ 27 cells in 3-D). The distance weighted smoothing algorithm discussed in the work of Rausch [18] was implemented.
V.2 On the smoothed VOF field, evaluate the interface normal components.
V.3 Reconstruct the interface by PLIC technique, using the iterative method (bisection/ Regula Falsi) and evaluate the magnitude of interface area.
V.4 On the non smoothed VOF field, choose and mark the cells with VOF in the limit $10^{-6} \leq f_c \leq 1 - 10^{-6}$.
V.5 Based on the reconstructed interface, evaluate the gas side temperature gradients for the marked interface cells.

Downloaded by 184.186.21.165 on August 17, 2019 | http://arc.aiaa.org | DOI: 10.2514/6.2019-4415

V.6 Using the vaporization rate and interfacial area density, evaluate mass generation source term for the marked cells.
V.7 Apply the mass generation source term to the VOF equation of liquid (consumption) and vapor (generation).
V.8 Evaluate and apply the energy source term, which includes the effect of latent heat.

The smoothing of the VOF field is essential for accurate evaluation of the local surface normal and curvature, which was based on the work of Rausch [18]. The overall algorithm was implemented in a parallel UDF framework, provided in ANSYS- FLUENT.

From the reaction viewpoint, proper resolution of the turbulence and reaction time scales is essential. The conventional laminar Finite Rate Model (FRM) based on the Arrhenius reaction rate parameters and associated reactions considered were based on the work of Leccese [2]:

$$\begin{array}{ll} 1 & C_{32}H_{66} \longrightarrow 16C_2H_4 + H_2 \\ 2 & C_2H_4 + O_2 \longrightarrow 2\,CO + 2\,H_2 \\ 3 & C_2H_4 + 2\,H_2O \longrightarrow 2\,CO + 4\,H_2 \\ 4 & H_2+0.5O_2 \longleftrightarrow H_2O \end{array}$$

The Arrhenius reaction rate parameters, adapted from the work of Coronetti et. al [12], for the above listed reactions are:

$$\begin{aligned} v_1 &= 3.09X10^{13}T^0 \exp(29790.6/T)\,[C_{32}H_{66}] \\ v_2 &= 9.11X10^{13}T^0 \exp(15702.1/T)\,[C_2H_4]^{0.5}\,[O_2]^{1.25} \\ v_3 &= 3.48X10^{11}T^0 \exp(15400.1/T)\,[C_2H_4]\,[H_2O] \\ v_4 &= 2.8X10^{18}T^{-1} \exp(21691/T)\left([H_2O] - \frac{[H_2][O_2]^{0.5}}{K_e}\right) \end{aligned}$$

The finite rate modeling leads to a stiff system of non linear equation, with a requirement for a stiff ODE solver (having time scales of the order of $\approx 10^{-8}$). In turbulent flow problems the reaction rate is limited by the mixing time scale which can be determined from the turbulent scales. The Eddy dissipation methodology, based on the work of Magnussen et. al [19], is based on local turbulent scale and concentration values, related together by empirical constants. It has much faster and stable convergence behavior. However, the Eddy Dissipation model (EDM) is effective for single step reaction mechanisms and would lead to inaccurate results for reaction mechanisms involving reversible reaction steps. To understand the effectiveness of using (EDM), a simple stochiometric reaction for the combustion of Paraffin was assumed.

$$C_{32}H_{66} + 48.5\,O_2 \longrightarrow 32\,CO_2 + 33H_2O$$

From the literature [16], it is understood that the effective single step reaction would be combustion of ethylene (through cracking of heavy Paraffins). However it was noticed that such direct ethylene reaction is difficult to implement in the current frame work, which involves both melting and vaporization of paraffin wax, justifying the use of above reaction. A completely coupled (combustion with melting) case without using any assumptions was modelled in fluent. This essentially involved, a solid paraffin modeled in the flow domain, with the outside surface undergoing vaporization and melting. The cases suffered from following difficulties:

- The mass continuity equations showed oscillatory convergence, taking large number of iterations to reach the expected convergence limits
- The temperature field showed artificial non-physical temperature rise, reducing the reliability of subsequent transient solutions.
- For ignition, a high temperature zone was patched near the leading edge of the Paraffin. However, this either caused unphysical temperature rise and reaction rates or the combustion was unsustained due to spatially non uniform vaporization rates.
- Owing to a large set of governing equations the computational time was significantly high.

To overcome the intractable nature of the problem, the system was decoupled into separate parts involving combustion and melting. A combustion problem was solved in an approximate domain representing the initial interfaces of the problem. The vaporizing interface was replaced by the solid wall, with appropriate mass, momentum and energy source term being added to the cell adjacent to the wall [2]. The heat, mass and species balance was carried out at the wall.

Downloaded by 184.186.21.165 on August 17, 2019 | http://arc.aiaa.org | DOI: 10.2514/6.2019-4415

The species balance at the interface was evaluated as,

$$\dot{m} = \frac{\rho_{\mathrm{g}} \mathrm{D}_{\mathrm{g}} \nabla_n \{\mathrm{Y}_{\mathrm{f}}\}}{1 - \mathrm{Y}_{\mathrm{sat}}} \tag{1}$$

Based on the previous works on vaporization [20],the condition at the wall was assumed to be saturated and the saturation mass fraction at the interface, was evaluated by assuming a linear relationship between temperature and mass fraction as given by equation Eq.(2).

$$\mathrm{Y}_{\mathrm{sat}} = (\mathrm{T} - \mathrm{T}_{\mathrm{m}})/(\mathrm{T}_{\mathrm{v}} - \mathrm{T}_{\mathrm{m}}) \tag{2}$$

where in the suffix 'v' and 'm' represents boiling point and melting point respectively. Ideally, a relationship between saturation pressure ($\mathrm{P}_{\mathrm{sat}}$) and given surface temperature ("Antoine" kind equation), for paraffin, example as given in the work of Riazi [21], needs to be utilized and the saturation mass fraction, for a single species fuel, is expressed as a ratio of vapor pressure ($\mathrm{P}_{\mathrm{sat}}$) and the corresponding operating pressure (P_{op}). However the equation provided in [21], tends to provide high surface temperature on the wall, which led to the assumption of an alternate linear system.

The energy balance at the vaporizing interface was taken as

$$\kappa_l \left.\frac{\partial \mathrm{T}}{\partial \mathrm{n}}\right|_{\mathrm{l}} - \kappa_s \left.\frac{\partial \mathrm{T}}{\partial \mathrm{n}}\right|_{\mathrm{s}} = \dot{m}\mathrm{L}_{\mathrm{v}} \tag{3}$$

In the above equation the suffix 'l' represents gas side/ liquid side gradients and suffix 's' represents the liquid side/solid side gradients for vaporization and melting respectively. As mentioned earlier, for the decoupled approach the wall is treated as the melting interface and the rate of heat removal from the interface due to the presence of the liquid film in the case of liquefying fuels is modelled by assuming appropriate thickness for the liquid film. In case of a planar geometry, where in the normal coordinate is represented by the y direction, the discretized surface species and energy balance is given by:

$$\dot{m} = \frac{\rho_g \mathrm{D}_{\mathrm{g}}}{1 - \mathrm{Y}_{\mathrm{sat}}} \frac{(\mathrm{Y}_{\mathrm{c}} - \mathrm{Y}_{\mathrm{s}})}{\delta y} \tag{4}$$

$$\dot{m} = \kappa_l \left.\frac{(\mathrm{T}_{\mathrm{c}} - \mathrm{T}_{\mathrm{s}})}{\delta y_l}\right|_{\mathrm{l}} - \kappa_s \left.\frac{(\mathrm{T}_{\mathrm{s}} - \mathrm{T}_{\mathrm{m}})}{\delta y_s}\right|_{\mathrm{s}} \tag{5}$$

where Eq.4 is used for solving the liquid surface regression rate and the Eq.5 is used for evaluating the surface temperature. The thickness of the liquid film δ_s is appropriated from empirical correlation of Karaybeyoglu [5] and corrected in an iterative manner based on the results from the melting problem. The combustion part of the problem provides following output:

- Boundary flame location
- Liquid surface vaporization rate (regression) and temperature distribution.
- Species, thermal and velocity boundary layer profiles.

The vaporization rate and temperature distribution from the combustion part of the problem is imposed on the free liquid surface of the melting problem. In the melting problem, similar to the coupled approach, a frozen material is patched inside a appropriate fluid domain. For ease of determining the liquid layer surface, a small liquid film is patched over the frozen material. The temperature and regression rates are applied using appropriate source terms through the user defined function. The liquid layer over the solid surface is tracked at all time points and the source terms are continuously imposed. The local interfacial area of the liquid surface is evaluated using the (V1-V4).An explicit VOF technique, based on PLIC in ANSYS-Fluent, convects the liquid surface, based on local velocity components. In case of combustion, a momentum source component was imposed as the wall normal is well defined in all times. For simulating vaporization in the melting problem, only mass source was imposed.

III. Case Study

An experimental study of quantification of spatial regression rate for the combustion of Paraffin wax, carried out by Dunn et. al. [22], was chosen to validate the decoupled approach and implementation. The computational domain and boundary conditions are shown in Fig.2.

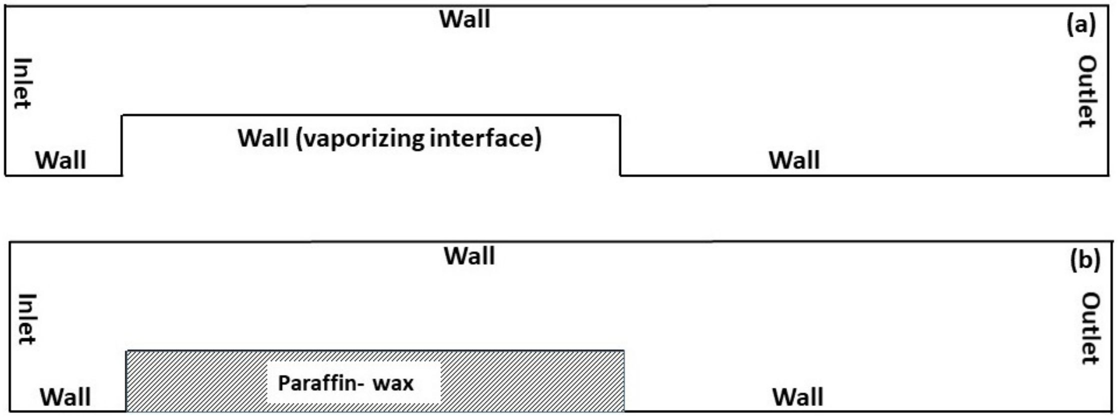

Fig. 2 Computational Domain (a) combustion problem (b) Melting problem

No slip constant temperature condition was imposed on the wall. The pertinent values of the constants, including the spatial dimension is given in Table.2. The actual experimental set up included a long duct to provide a fully developed turbulent inlet conditions. To reduce the computational effort, a steady state turbulent analysis was carried out on the actual domain, with a step near the exit, simulating the presence of solid paraffin. From the velocity field , the profile at appropriate location (~ 1.8m from the inlet) is extracted and was used as inlet conditions for the combustion and melting problems. The flow domain was of ~ 2m, while the combustion and melting computations were carried out inside a domain of 0.165 m in length, which is a significant reduction in the computational effort.

PARAMETER	**INPUT VALUES**
Dimension(Domain) [mm]	L=165, H=25.4
INITIAL CONDITIONS	
Dimension(Fuel slab) [mm]	L_m=73 & H_m=9
Subcool [K]	≈ 40
Temp. diff. btw phases [K]	≈ 0
BOUNDARY CONDITIONS	
Oxidizer mass flux $\left[\frac{kg}{m^2-s}\right]$	G_o= 8&14

Table 2 Input parameters for validation

Numerical aspect	**Method**
Gradient evaluation	Gauss cell centered
Convective term	Second order upwind method
Diffusive term	Central difference
Pressure velocity coupling	SIMPLEC
Pressure interpolation	PRESTO
Combustion	Stiff ODE solver with ISAT

Table 3 Choice of solvers

From the choice of solvers available in ANSYS-Fluent,the combination shown in Table. 3, provided faster and stable convergence. For combustion, ISAT algorithm with intermediate Direct integration, based on data storage and solution mapping, provided significant acceleration in convergence over using only Direct integration Stiff solver.

The material properties for paraffin wax, used in this simulation Table.4,were mostly taken from the work of Karabeyoglu [5]. The temperature dependence of thermal properties and flow properties was neglected. The liquid expansion, typical in paraffin wax, was neglected, using the same density for solid and liquid phases. The constant value of thermal diffusivity of $6\text{x}10^{-5}\text{m}^2/\text{s}$ was employed. The density of paraffin gas vapor was taken close to other higher hydrocarbon gas densities. The other gases and its properties were assumed to have constant standard values. Incompressible ideal gas relation was used for species density, where in the the actual pressure in the ideal gas was replaced with the operating pressure, which in the present case study is atmospheric pressure.

IV. Preliminary Results

The contour plot of temperature distribution given in Fig.3 clearly shows the position of the flame in the boundary layer adjacent to the vaporizing interface (wall). The temperature distribution and regression rate along the direction of the melting surface provided in the Fig.4, serves as an input for the melting part of the problem. For both the combustion modeling approaches, the problem with higher oxidizer influx has the higher regression rates. The eddy dissipation

Downloaded by 184.186.21.165 on August 17, 2019 | http://arc.aiaa.org | DOI: 10.2514/6.2019-4415

Physical property	**Value**	
	Paraffin liquid/ Solid	Gas
Density [kg/m^3]	700	7
Thermal conductivity [W/(m.K)]	0.12	0.05
Viscosity [Pa.s]	$6.5X10^{-4}$	$4X10^{-5}$
Standard heat of formation (J/kmol)	-16x10^8	
Surface Tension [N.m]	0.07	
Melting point [K]	340	
Heat of fusion [kJ/kg]	167.2	
Heat of vaporization [kJ/kg]	163.5	

Table 4 Physical properties used in the simulation

model provides a consistent increase of regression rate in the flow direction, while in finite rate modeling, there is a increase followed by a slight decrease in the regression rate. This result can be understood using previous research data [1] [2] [22]. Such near leading edge fluctuations in the regression rates were noticed in the work of Dunn et. al [22]. The increased mass flow rate along the flow direction causes an increase in regression rate. However during the initial part of the melting, there is competing effects of increased mass flow rate and boundary layer effects. Secondly, it was observed that as the finite rate modeling was used, without any inclusion of turbulent effects in combustion, similar to the work in [2], there was fluctuation in the flame position along the flow direction, which could be caused by the turbulent nature of the flow. This turbulent fluctuations persisted in the region of study and was susceptible to divergence during multiple restarts of the solver.

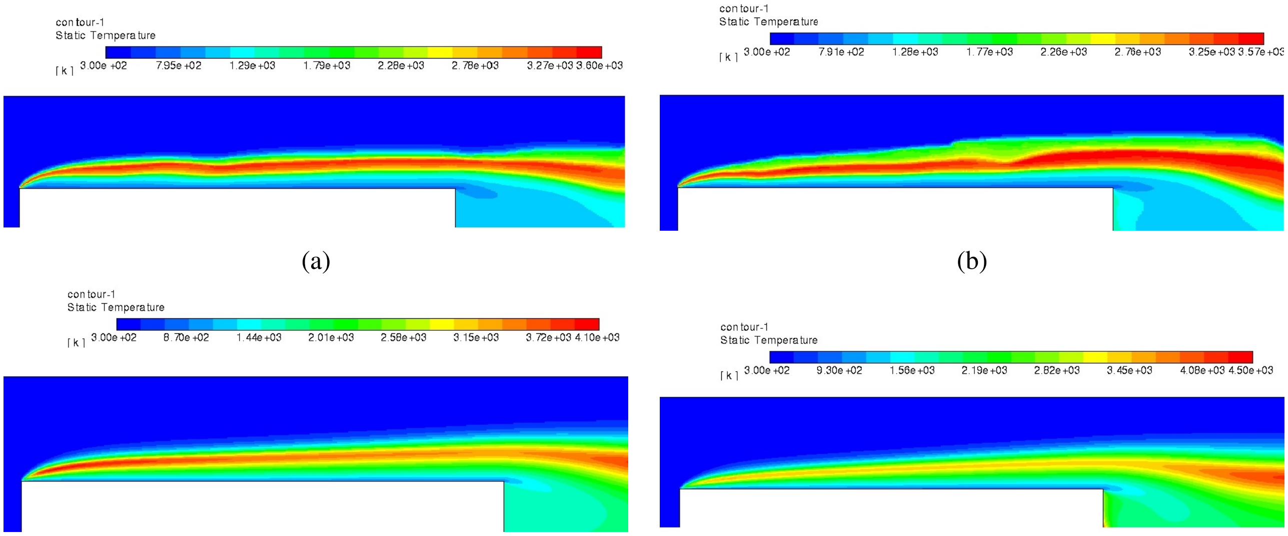

(a) (b)

(c) (d)

Fig. 3 (a) & (b) Temperature contours for G_o of 8 and 14 kg/m^{2}s using finite rate model, (c) & (d) Temperature contours for G_o of 8 and 14 kg/m^{2}s using Eddy dissipation model

The spatially averaged regression rates obtained by two combustion models were compared with the experimental results in Table [5]. It was noticed that the Finite Rate modeling results were very close to that observed in the experiments. This meets the expectations, as the FRM model employs more detailed chemical mechanism when compared to the eddy dissipation model. It also highlights, as mentioned earlier, the inability of eddy dissipation model to handle multiple reaction steps, especially those having reversibility.

Downloaded by 184.186.21.165 on August 17, 2019 | http://arc.aiaa.org | DOI: 10.2514/6.2019-4415

Downloaded by 184.186.21.165 on August 17, 2019 | http://arc.aiaa.org | DOI: 10.2514/6.2019-4415

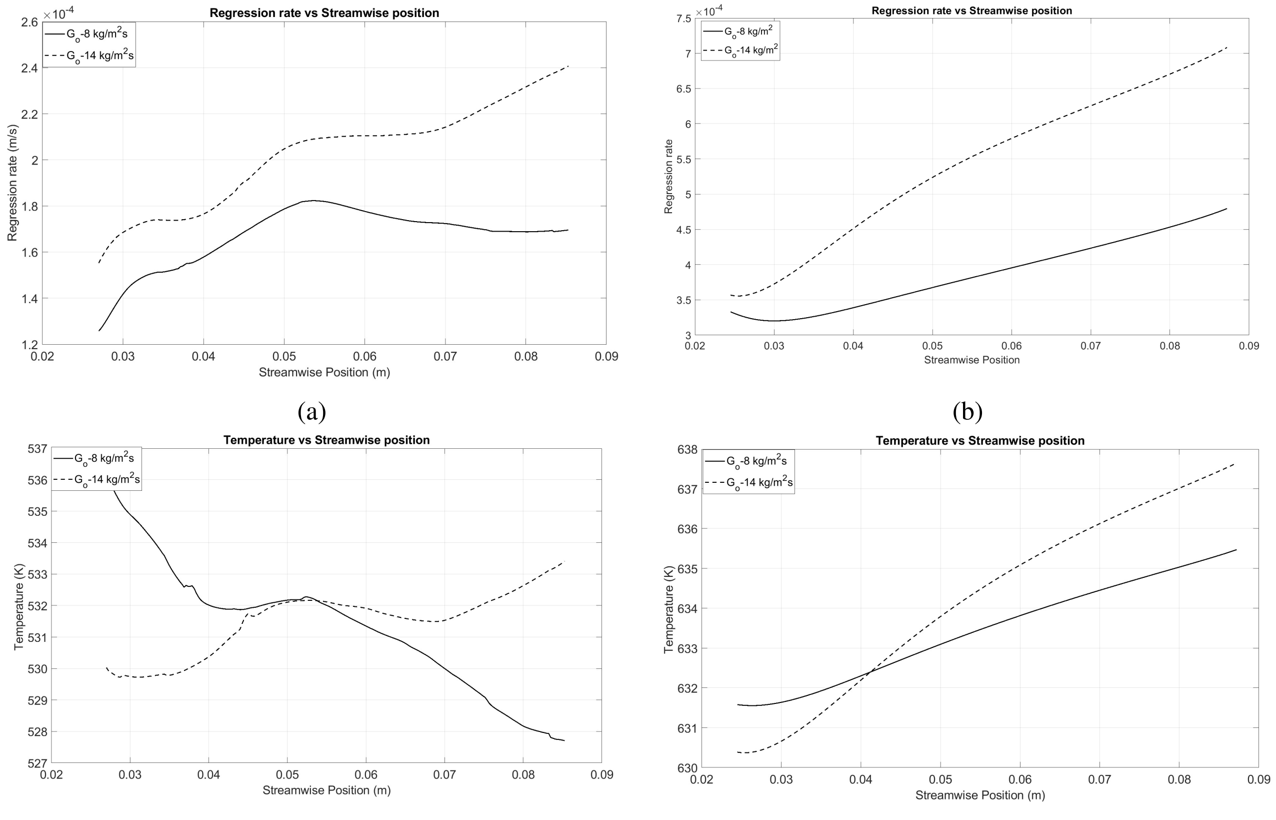

(a)

(b)

(c)

(d)

Fig. 4 (a) & (b) Stream wise variation of regression rate using FRM & EDM , (c) & (d) Stream wise variation of temperature using FRM & EDM

One effective technique to overcome this shortcoming would be employing the Eddy Dissipation Concept (EDC) [23]. The crux of EDC is to mark probable candidate computational cells for combustion and treat each marked cell as a Partially Stirred reactor.This ensures the inclusion of detailed chemical mechanisms while including the turbulent mixing effects.During the future course of this research, a detailed analysis on EDC with a vaporizing interface would be carried out.

There is reduced temperature variation along the vaporizing surface. The detailed FRM predicts lesser temperature in comparison to the EDM in Fig.5. This is could be caused by the endothermic reaction-Paraffin cracking into Ethylene, occurring very close to the vaporizing surface of the liquid melt .The peak flame temperature of the two models are comparable, while EDM model predicts the highest peak temperature.The combustion study reiterates the importance of employing relevant detailed chemical mechanisms.

The temperature distribution obtained and the regression rates obtained from the combustion problem, was applied to the melting paraffin wax interface, using algorithm detailed in previous sections. The temperature and regression distribution obtained from both the combustion problems were employed and the $G_o = 14\text{kg}/\text{m}^2\text{s}$ was used as the inflow condition. During the initial melting, the melting rates were high, corresponding higher initial temperature gradients.

Mass flux (G_o($\text{kg}/\text{m}^2\text{s}$))	8	14
Experimental [mm/s]	0.17	0.27
Numerical (FRM) [mm/s]	0.144	0.21
Numerical (EDM) [mm/s]	0.3875	0.525

Table 5 Comparison of regression rates : Experimental and Numerical

Downloaded by 184.186.21.165 on August 17, 2019 | http://arc.aiaa.org | DOI: 10.2514/6.2019-4415

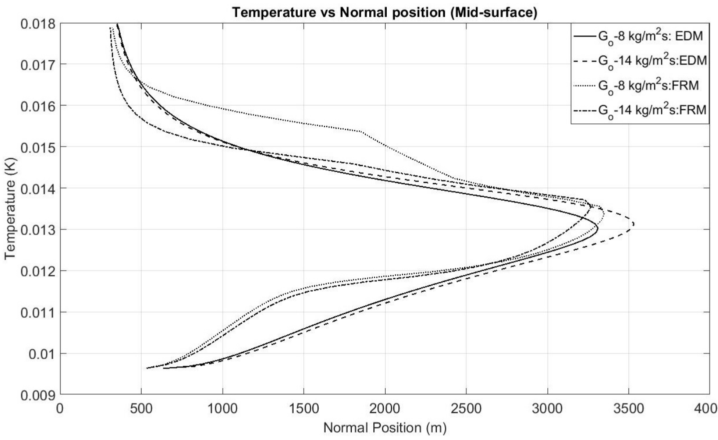

Fig. 5 Temperature distribution in the direction normal to the meting interface

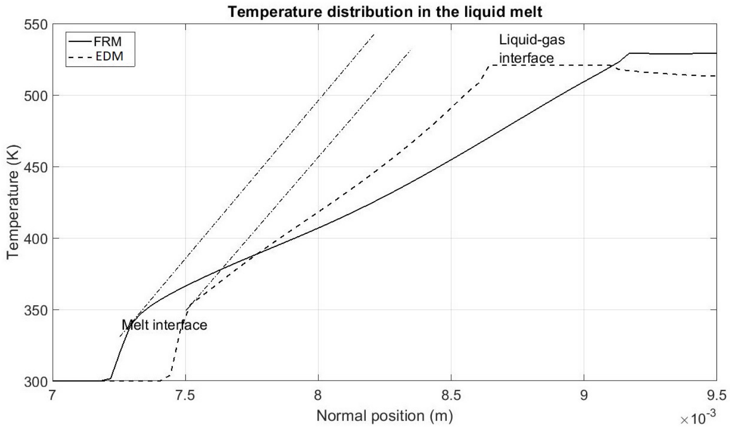

Fig. 6 Temperature variation along the liquid melt film thickness

During the subsequent time steps the solution reached a steady state, with effective melt thickness being a constant at different time points. However this steady state melt rate was 2 order higher ($4 - 10$mm/s) when compared to the experimental results of (0.2mm/s). To isolate the cause of this aberration, the surface temperature was artificially reduced to values of (450, 400, 375 K). It was noticed that for all the listed interface temperature values, the melting rates were higher than that observed in the case of the experiments. Subsequently the temperature distribution across the liquid film was analyzed. The temperature distribution across the film was taken at the mid surface stream wise location as shown in Fig.6

The melt surface and the melt film liquid surface location has been marked for clarity. The perceived temperature gradient at the melt interface has been marked as a tangent to the melt interface location. It can be noticed that the gradient at the melt interface is greater than the linear temperature gradient that can be obtained from the melt surface temperature and melt film thickness values. This observation can be attributed to the convective effects near the melting interface. From the problem formulation viewpoint, two assumptions in the problem could cause the deviation.The density difference between the solid and the liquid phase was neglected, which is of significant magnitude in the case of the Paraffin wax. Lower liquid density would cause a bulk flow at the melting interface, with the normal direction flow having an effect of reducing the temperature gradient, as discussed in [24]. Secondly, the liquid viscosity was considered as a temperature invariant quantity in the problem. However in the work of Leccese [2], it was shown that in the given operating range the viscosity varies in the range of ($6X10^{-4}$ to $9X10^{-3}$). The viscosity variation as a function of temperature, based on the governing transcendental equation in [2], is shown in the Fig.7.

Increased viscosity at reduced temperatures, as experienced near the melting interface, reduces the convective and entertainment effects, lowering the spatially averaged melting rates. The effects of temperature varying viscosity and

Downloaded by 184.186.21.165 on August 17, 2019 | http://arc.aiaa.org | DOI: 10.2514/6.2019-4415

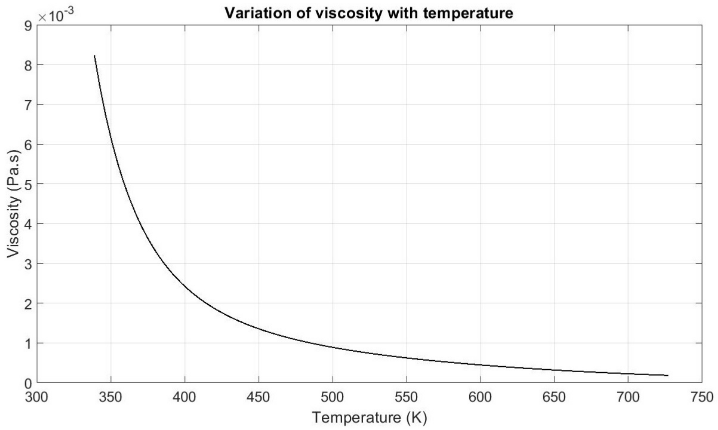

Fig. 7 Variation of viscosity with temperature

density needs to be studied in detail.

The representative results, showing the transfer of information from the combustion model and the surface instabilities captured by the multiphase model, is provided in Fig.8. Though qualitative in nature, the contours clearly show the significance of droplet entrainment in a combustion problem. Also, the liquid surface was resolved and it was found that the there was 10% increase in the available surface area, over that of a unperturbed interface. A representative melt interface deformation as function of unperturbed position is provided in Fig.9. As highlighted in the work of Karabeyoglu[5] & Gater [7], apart from entrainment effects, the increased surface roughness is important factor for the increased regression rates observed in the case of liquefying fuels.

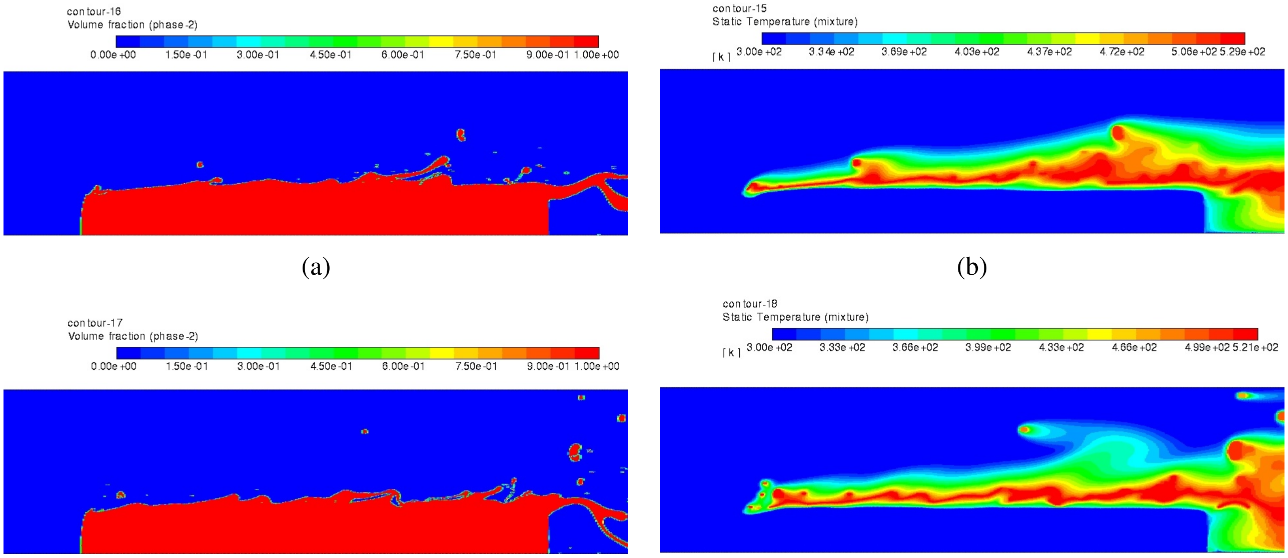

(a) (b)

(c) (d)

Fig. 8 (a) & (b) Contour plots of Phase and temperature for EDM based surface temperature input (G_o= 14 kg/m^{2}s) , (c) & (d) Contour plots of Phase and temperature for FRM based surface temperature input (G_o=14 kg/m^{2}s)

This present decoupled methodology offers the following advantage over previous approaches:

1) Remove the requirement of employing empirical regression relation.
2) No assumption needs to be made for the temperature distribution in the solid and liquid region.
3) The empirical correlation for surface roughness and entrainment effects can be removed.

Downloaded by 184.186.21.165 on August 17, 2019 | http://arc.aiaa.org | DOI: 10.2514/6.2019-4415

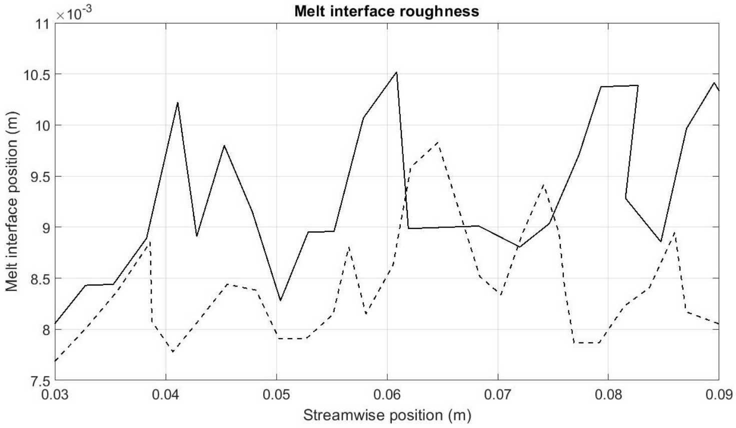

Fig. 9 Reconstructed liquid surface roughness caused by instability

4) More realistic entrainment rate prediction can be made for domain of arbitrary initial shape.

However, the present approach will suffer from some shortcomings of the previous methods, which are:

- The effect of liquid surface irregularity on the position of flame cannot be quantified, as the ideal vaporizing surface is assumed for the combustion problem.
- The effect of regressing fuel surface on the flow, and hence the combustion, cannot be quantified, as the vaporizing surface in the combustion problem is assumed to be fixed.

The last shortcoming can be slightly alleviated by understanding the time history of the melt surface location (in the melting problem) and setting the vaporizing surface (combustion problem) in the combustion problem at respective representative locations, between start and end of melting. This is very similar to the approach used in the work of Venkateswaran et. al [8].

V. Conclusion

A novel methodology for conducting transient numerical analysis of hybrid propulsion was discussed, by decoupling the combustion and the melting phase change problems. As a case study, the experimental combustion of a paraffin wax slab was simulated. Two combustion models were employed to understand the requirement of any detailed reaction steps. It was noticed that the Finite Rate Modeling (FRM) with detailed mechanisms provided accurate results over a single step mechanism used in the EDM technique. However, due to turbulence, FRM technique showed convergence instabilities and solution oscillations , with a necessity of considering EDC as an alternate combustion model. A successful temperature and regression rate mapping technique was implemented in the melting problem. However with the prescribed surface temperatures, the melting problem predicted unrealistically high melting rate. Upon detailed analysis, temperature dependent density and viscosity is being considered as the probable cause for the aberration. In the future work, the temperature dependency of thermal and flow properties would be considered in detail. Also from the work of Leccese[2], it was noticed that radiation played a significant role (due to the presence of absorbing/emitting medium). In subsequent research efforts, a suitable radiation model would be included and the effect of radiation heat flux on melting and vaporization will be considered.

Acknowledgements

This research was made possible by the Economic Development Assistantship (EDA) provided by the graduate school of Louisiana State University (LSU).

References

[1] Kuo, K. K., and Chiaverini, M. J., *Fundamentals of hybrid rocket combustion and propulsion*, American Institute of Aeronautics and Astronautics, 2007.

Downloaded by 184.186.21.165 on August 17, 2019 | http://arc.aiaa.org | DOI: 10.2514/6.2019-4415

[2] Leccese, G., Bianchi, D., and Nasuti, F., "Modeling and Simulation of Paraffinâ€"Based Hybrid Rocket Internal Ballistics," *2018 Joint Propulsion Conference*, 2018, p. 4533.

[3] Larson, C., DeRose, M., Pfeil, K., Carrick, P., DeRose, M., Pfeil, K., Carrick, P., and Larson, C., "Tube burner studies of cryogenic solid combustion," *33rd Joint Propulsion Conference and Exhibit*, 1997, p. 3076.

[4] Gramer, D., Knuth, W., Rice, E., and St. Clair, C., "Experimental investigation of a metallized cryogenic hybrid rocket engine," *34th AIAA/ASME/SAE/ASEE Joint Propulsion Conference and Exhibit*, 1998, p. 3509.

[5] Karabeyoglu, M., Altman, D., and Cantwell, B. J., "Combustion of liquefying hybrid propellants: Part 1, general theory," *Journal of Propulsion and Power*, Vol. 18, No. 3, 2002, pp. 610–620.

[6] Karabeyoglu, M., and Cantwell, B. J., "Combustion of liquefying hybrid propellants: Part 2, Stability of liquid films," *Journal of Propulsion and Power*, Vol. 18, No. 3, 2002, pp. 621–630.

[7] Gater, R. A., and L'Ecuyer, M. R., "A fundamental investigation of the phenomena that characterize liquid-film cooling," *International Journal of Heat and Mass Transfer*, Vol. 13, No. 12, 1970, pp. 1925–1939.

[8] S.Venkateswaran, C., "Size scale up in hybrid rocketv motors," *AIAA meeting papers*, Vol. 34th Aerospace Sciences Meeting and Exhibit, No. -, 1996, pp. –.

[9] Cheng, G., Farmer, R., Jones, H., and McFarlane, J., "Numerical simulation of the internal ballistics of a hybrid rocket motor," 1994. doi:10.2514/6.1994-554.

[10] Serin, N., and Yalcin, G., "Navier-Stokes Investigation on Reacting Flow Field of HTPB/O2 Hybrid Motor and Regression Rate Evaluation," 2003. doi:10.2514/6.2003-4462.

[11] Knuth, W., Gramer, D., Chiaverini, M., Sauer, J., Whitesides, R., and Dill, R., "Preliminary CFD analysis of the vortex hybrid rocket chamber and nozzle flow field," *34th AIAA/ASME/SAE/ASEE Joint Propulsion Conference and Exhibit*, 1998, p. 3351.

[12] Coronetti, A., and Sirignano, W. A., "Numerical analysis of hybrid rocket combustion," *Journal of Propulsion and Power*, Vol. 29, No. 2, 2013, pp. 371–384.

[13] Petrarolo, A., Kobald, M., and Schlechtriem, S., "Liquid Layer Combustion Visualization of Paraffin-Based Hybrid Rocket Fuels," *53rd AIAA/SAE/ASEE Joint Propulsion Conference*, 2017, p. 4828.

[14] T. Jens, E., A. Chandler, A., Cantwell, B., Scott Hubbard, G., and Mechentel, F., "Combustion Visualization of Paraffin-Based Hybrid Rocket Fuel at Elevated Pressures," 2014. doi:10.2514/6.2014-3848.

[15] Chandler, A., Jens, E., Cantwell, B., and Hubbard, G. S., "Visualization of the liquid layer combustion of paraffin fuel for hybrid rocket applications," *48th AIAA/ASME/SAE/ASEE Joint Propulsion Conference & Exhibit*, 2012, p. 3961.

[16] Ranuzzi, G., Cardillo, D., and Invigorito, M., "Numerical Investigation of a N2O-Paraffin Hybrid Rocket Engine Combusting Flowfield," *6th European Conference for Aeronautics and Space Sciences (EUCASS), Krakow, Poland*, 2015.

[17] Scheufler, H., and Roenby, J., "Accurate and efficient surface reconstruction from volume fraction data on general meshes," *Journal of Computational Physics*, Vol. 383, 2019, pp. 1 – 23. doi:https://doi.org/10.1016/j.jcp.2019.01.009, URL `http://www.sciencedirect.com/science/article/pii/S0021999119300269`.

[18] RAUSCH, R., YANG, H., and BATINA, J., "Spatial adaption procedures on unstructured meshes for accurate unsteady aerodynamic flow computation," *32nd Structures, Structural Dynamics, and Materials Conference*, 1991, p. 1106.

[19] Magnussen, B., and Hjertager, B., "On mathematical modeling of turbulent combustion with special emphasis on soot formation and combustion," *Symposium (international) on Combustion*, Vol. 16, Elsevier, 1977, pp. 719–729.

[20] Tanguy, S., Ménard, T., and Berlemont, A., "A Level Set Method for vaporizing two-phase flows," *Journal of Computational Physics*, Vol. 221, No. 2, 2007, pp. 837 – 853. doi:https://doi.org/10.1016/j.jcp.2006.07.003, URL `http://www.sciencedirect.com/science/article/pii/S0021999106003214`.

[21] Riazi, M. R., and AlQaheem, Y. S., "Predicting Vapor Pressure of Heavy Hydrocarbons from Molar Refraction and Its Applications to Petroleum Mixtures," *Industrial & Engineering Chemistry Research*, Vol. 49, No. 15, 2010, pp. 7104–7112. doi:10.1021/ie100861c, URL `https://doi.org/10.1021/ie100861c`.

[22] Dunn, C., Gustafson, G., Edwards, J., Dunbrack, T., and Johansen, C., “Spatially and temporally resolved regression rate measurements for the combustion of paraffin wax for hybrid rocket motor applications,” *Aerospace Science and Technology*, Vol. 72, 2018, pp. 371 – 379. doi:https://doi.org/10.1016/j.ast.2017.11.024, URL `http://www.sciencedirect.com/science/article/pii/S1270963816311002`.

[23] Magnussen, B., “On the structure of turbulence and a generalized eddy dissipation concept for chemical reaction in turbulent flow,” *19th aerospace sciences meeting*, 1981, p. 42.

[24] Shyy, W., *Computational Modeling for Fluid Flow and Interfacial Transport (Dover Books on Engineering)*, Dover Publications, Inc., New York, NY, USA, 2006.

Downloaded by 184.186.21.165 on August 17, 2019 | http://arc.aiaa.org | DOI: 10.2514/6.2019-4415